Generation of unipolar electromagnetic pulses in semiconductor nanocrystals

M. M. Glazov ● and N. N. Rosanov ●
Ioffe Institute, 194021 St. Petersburg, Russia

We show that excitation of a semiconductor nanocrystal with a short pulse of electromagnetic field can result in the generation of a unipolar electric pulse, which is the distribution of field with a nonzero electric pulse area. The effect is caused by the exciton nonlinearity in a nanocrystal. The microscopic theory of the effect is presented. We also discuss related proposals of unipolar pulse generation, including the optical rectification effect and electric field-induced interband ionization of a nanocrystal.

I. INTRODUCTION

In recent decades, impressive progress has been made in obtaining increasingly shorter electromagnetic (optical) pulses, marked by the awarding of Nobel Prizes in 1999 for the use of femtosecond laser pulses to study the motion of atoms in molecules and in chemical reactions [1], and in 2023 for methods of generation and application of attosecond (as) (1 as = 10^{-18} s) pulses [2]. The already achieved pulse duration of 43 as [3] is noticeably shorter than the Bohr period of electron revolution around the nucleus of a hydrogen atom; there are proposals for obtaining even shorter pulses. This opens up the opportunity to "look inside the atom," that is, to trace the manifestations of the intra-atomic movement of electrons. An important issue for such short pulses is the effectiveness of their impact on micro-objects. A large number of works [4–14] show that this efficiency depends significantly on the electrical pulse area

$$S_E = \int_{-\infty}^{\infty} E(t)dt, \qquad (1)$$

where E is the electric field strength and t is time. Indeed, pulses with a nonzero electric area, which we call unipolar, have a unidirectional effect on charges, in contrast to the multidirectional effect of bipolar pulses.

Currently obtained attosecond pulses are multicycle; their electrical area is close to zero due to multiple oscillations of the electric field. Unipolar electromagnetic pulses have been obtained experimentally in a number of works [15–21]; there are various proposals for more effective methods for their generation; see, e.g., Refs. [22,23].

Still, it is highly desirable to have a compact source of unipolar pulses that is compatible with current technological platforms. In this respect, application of semiconductor nanosystems, particularly nanocrystals, also known as quantum dots, seems beneficial. Since their discovery [24–26], nanocrystals have been actively studied both from technological and physical standpoints [27–29]. Their fascinating electronic, spin, and optical properties [30–35] pave the way to various applications, including those in nonlinear optics [36,37] and attosecond physics [38,39].

The aim of this paper is to analyze the possibility of converting zero-area pulses into unipolar ones using the nonlinear response of semiconductor nanocrystals. We show that a multicycle pulse with zero electric area can be converted by a nanocrystal to a unipolar pulse of a sizable magnitude. After brief introduction, in Sec. II we present a model of a nanocrystal as a nonlinear oscillator, provide a general expression for the spatial distribution of the electrical area of a driven nanocrystal, and show the possibility of obtaining a pulse with a nonzero area with the proper driving pulse shape. Numerical results are also presented here for a realistic shape of driving pulses when varying the parameters of a nanocrystal with cubic nonlinearity in a wide range. In Sec. III, we provide estimates of quantities, and we discuss the case of nanocrystals with quadratic nonlinearity and the achievability of experiments. The main findings are summarized in Sec. IV.

II. THEORY

A. Model

We consider a semiconductor nanocrystal (quantum dot) subject to the propagating electromagnetic field $E_i(t)$ (Fig. 1) in the form of the zero-area pulse, $S_{E,i} \equiv \int_{-\infty}^{\infty} E_i(t)dt = 0$ [cf. Eq. (1)]. This means vanishing of a zero-frequency component of the pulse spectrum. The size of the nanocrystal is typically much smaller than the light wavelength, thus we disregard the coordinate dependence of the incident field and consider its interaction with the nanocrystal in the dipole approximation. In what follows, we assume for simplicity that the field is linearly polarized along one of the main crystalline axes of the nanocrystal, e.g., along the x-axis. This allows us to take into account only the x-components of the field and dielectric polarization in the nanocrystal, consequently we omit Cartesian subscripts in what follows.

We describe the exciton polarization in a quantum dot that arises due to the transition of an electron from the valence band to the conduction band within a nonlinear oscillator model in the form [31,40]

$$\ddot{d} + 2\gamma\dot{d} + \omega_0^2 d + \beta d^3 = \lambda(1 - \xi d^2)E_i(t), \qquad (2)$$

where $E_i(t)$ is the incident field, $d \equiv d(t)$ is the time-dependent dipole moment of the exciton, dots denote the
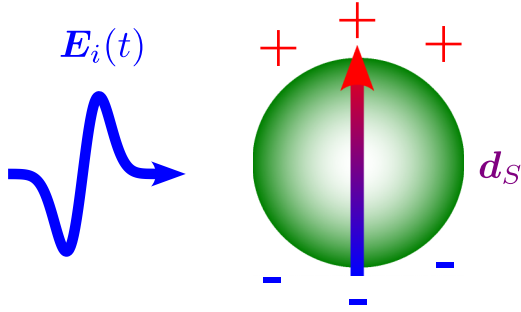
FIG. 1. Schematics of the proposed effect. The nanocrystal (green ball) is subject to a zero-area electromagnetic pulse $\boldsymbol{E}_i(t)$. As a result of the temporary separation and subsequent merging of negative and positive charges in the nanocrystal, a temporal profile of the dipole moment with a nonvanishing zero-frequency component $\boldsymbol{d}_S \neq 0$ is formed, which serves as a source of a unipolar electromagnetic pulse.

time derivatives, $\omega_0 = (E_g - E_b)/\hbar$ is the exciton resonance frequency with E_g and E_b being the quantum dot band gap and exciton binding energy, respectively, and $\gamma > 0$ is the exciton damping rate that includes both radiative and nonradiative recombination processes; the physical meaning and microscopic expressions for the nonlinearity coefficients, β and ξ, and the exciton-field coupling constant, λ, will be specified below. Note that the field that appears as a result of radiative decay has a zero electric area, and it plays no role in what follows. The extension of the model to fully account for a reduced symmetry of a nanocrystal is straightforward: one has to allow for an anisotropy of the restoring force and dipole field coupling. It does not bring novel physics in the case of cubic nonlinearity considered here, but becomes important if other effects, related, e.g., to quadratic nonlinearity, come into play; see Sec. III.

We recall that within a two-band model, the exciton dipole moment is related to the system parameters as [31,41]

$$d(t) = -C(t) \frac{i e p_{cv}}{\omega_0 m_0} \int \Phi^*(\boldsymbol{r}, \boldsymbol{r}) d^3 r + \text{c.c.} \tag{3}$$

Here $e < 0$ is the electron charge, p_{cv} is the interband momentum matrix element, m_0 is the free-electron mass, $\Phi(\boldsymbol{r}, \boldsymbol{r})$ is the smooth envelope of the exciton wave function taken at coinciding electron and hole coordinates $\boldsymbol{r}_e = \boldsymbol{r}_h \equiv \boldsymbol{r}$, $C(t)$ is the decomposition coefficient of the nanocrystal state as $|0\rangle + C(t)|\text{exc}\rangle$, where $|0\rangle$ is the ground state of the crystal and $|\text{exc}\rangle$ is the state where one exciton active in a given linear polarization is excited, and the integration in Eq. (3) is carried out over the nanocrystal volume. We introduce

$$\mathcal{D}_x = \left| \frac{e p_{cv}}{\omega_0 m_0} \int \Phi^*(\boldsymbol{r}, \boldsymbol{r}) d^3 r \right|, \tag{4}$$

which is the microscopic dipole moment of the exciton localized in a quantum dot: $\mathcal{D}_x$ gives the amplitude of the oscillating (at the resonant frequency ω_0) dipole induced by one exciton confined in a nanocrystal. The parameter $\lambda = 2\omega_0 \mathcal{D}_x^2/\hbar$ in Eq. (2) describes the coupling strength of the exciton with the electric field, and the coefficients β and ξ stand for the two key nonlinearities in the system: The constant β describes the nonlinearity related to the exciton energy shift due to the exciton-exciton interaction (also known

as the anharmonic oscillator nonlinearity), and the constant ξ describes the oscillator strength saturation effect (or the two-level system nonlinearity) [31,42]. The simplified form of the oscillator strength saturation nonlinearity, $1 - \xi d^2$, is valid for the polarization being much below its saturation value, $|\xi d^2| \ll 1$. The form of nonlinearity in Eq. (2) is quite generic and it is not related to a particular type of semiconductor, its crystalline symmetry, or the shape of the nanocrystal.

The parameters responsible for the nonlinearities depend on the nanocrystal parameters and, in particular, on the relation between the quantum dot size a and the exciton Bohr radius a_B in the bulk material, which also governs the exciton statistics [43]. For $a \ll a_B$ (small quantum dots), the Coulomb correlations between the electrons and holes are negligible [44,45], and the exciton forms a natural two-level system. In that case, $\beta \to 0$ and the oscillator strength saturation described by ξ dominates the nonlinear response. In the opposite limit where $a \gg a_B$, the exciton is localized in the quantum dot as a whole. In that case, the main nonlinearity results from exciton-exciton interactions, while ξ can be set to 0. In the following, we consider the latter case assuming that the quantum dot is sufficiently large [40,43], setting $\xi = 0$. Importantly, in this case the microscopic exciton dipole moment $\mathcal{D}_x$ is enhanced by a large factor $(a/a_B)^{3/2}$ (for spherical quantum dots) as compared to the "atomic" value of $|e p_{cv}/(m_0 \omega_0)|$ [46]. Thus, Eq. (2) reduces to the Duffing-like equation. While generally Eq. (2) is used to describe resonant or quasiresonant response [31], see also Refs. [42], it can be justified for sufficiently short incident pulses provided that the oscillator strengths of excited excitonic states are small compared to that of the ground state, as is usually the case [47] and if the details of the band structure, e.g., the presence of remote bands, is unimportant. Hence, Eq. (2) represents the simplest possible model to account for a nonlinear response of a nanocrystal. Note that the nonlinear Eq. (2) can also describe a response of small (subwavelength) dielectric or metallic nanoparticles in a single-mode approximation where the polarization can be related to the excitation of, respectively, Mie or plasmon modes [48–52]. For example, in the case of a plasmonic nanoparticle, the cubic nonlinearity in Eq. (2) is related to the action of ponderomotive force on the plasma [53,54].

We now show that the nonlinear dynamics of the exciton polarization given by Eq. (2) can give rise to a zero-frequency component of the exciton dipole moment,

$$d_S = \int_{-\infty}^{\infty} d(t) dt, \tag{5}$$

even if the incident pulse has no zero-frequency contribution,

$$\int_{-\infty}^{\infty} E_i(t) dt = 0. \tag{6}$$

The presence of $d_S \neq 0$ results in the unipolar electric pulse produced by the nanocrystal. Indeed, we use the explicit expression for the field produced by the oscillating dipole in the free space [55]:

$$\boldsymbol{E}(t) = \left[\left(\frac{3\boldsymbol{d}}{r^5} + \frac{3\dot{\boldsymbol{d}}}{cr^4} + \frac{\ddot{\boldsymbol{d}}}{c^2 r^3} \right) \cdot \boldsymbol{r} \right] \boldsymbol{r} \\ - \left(\frac{3\boldsymbol{d}}{r^5} + \frac{3\dot{\boldsymbol{d}}}{cr^4} + \frac{\ddot{\boldsymbol{d}}}{c^2 r^3} \right) \Bigg|_{t-r/c} \tag{7}$$

where r is the vector connecting the point where the field is measured and the center of a nanocrystal, and the values of the dipole d and its derivatives are taken at the earlier time $t' = t - r/c$. Integrating $E(t)$ over time, we obtain the electric pulse area in agreement with Ref. [23],

$$S_E = \frac{3(nd_S)n - d_S}{r^3}. \tag{8}$$

The part with nonzero pulse area corresponds to a combination of first terms, $1/r^3$, in each of the parentheses of Eq. (7), while the usual dipole radiation is related to the last, $1/r$, contributions. The expression (8) coincides with the dipole component of the far-field of a static system of electric charges [56]. Note that the electric pulse area decays as $1/r^3$ in free space. In different geometries, the decay can be suppressed; for instance, in coaxial waveguides without a cutoff frequency, the unipolar pulse can propagate conserving its shape [57].

It is instructive to demonstrate explicitly that Eqs. (7) and (8) are compatible with Gauss's law for electrodynamics. To that end, it is convenient to calculate the electric flux through a closed surface encompassing the nanocrystal:

$$\Phi_E(t) = \oiint E(t) \cdot dA, \tag{9}$$

where dA is the surface area element. In particular, integrating Eq. (9) over time, we obtain

$$\int_{-\infty}^{\infty} \Phi_E(t)dt = \oiint S_E \cdot dA \equiv 0, \tag{10}$$

where we explicitly used Eq. (8) for S_E. In fact, $\Phi_E(t)$ also vanishes as one can readily see from Eq. (7). (Derivation becomes particularly simple for a spherical surface, taking into account that the radial component of the field $E_r \propto \cos\theta$, where $\theta = \angle d_S, r$.) This is consistent with the fact that we do not have any free charges in the system. The charges in the nanocrystals separate in space only temporarily and on the distances $\lesssim a$ where a is the nanocrystal size to produce time-dependent $d(t)$. We discuss this issue in more detail in Appendix A.

To prove that the pulse with the zero electric area can generate a pulse with a nonzero area, let us rewrite Eq. (2) in the form

$$\lambda E_i(t) = \frac{1}{1 - \xi d^2}(\ddot{d} + 2\gamma\dot{d} + \omega_0^2 d + \beta d^3). \tag{11}$$

This equation shows which shape of the incident pulse $E_i(t)$ is required to form the exciton dipole moment profile $d(t)$. We now determine what restrictions the condition (6) imposes on the parameters of the pulse and the quantum dot to have $d_S \neq 0$. First, note that the magnitude of the damping term in Eqs. (2) and (11) does not affect the incident pulse electrical area at a given $d(t)$. Indeed, when integrating Eq. (11) over time, this term enters the electric pulse area as

$$\frac{2\gamma}{\lambda}\int_{-\infty}^{\infty} \frac{\dot{d}(t)}{1 - \xi d^2(t)}dt = \frac{\gamma}{\lambda\sqrt{\xi}}\ln\frac{1 + \sqrt{\xi}d(t)}{1 - \sqrt{\xi}d(t)}\bigg|_{t\to-\infty}^{t\to+\infty} = 0, \tag{12}$$
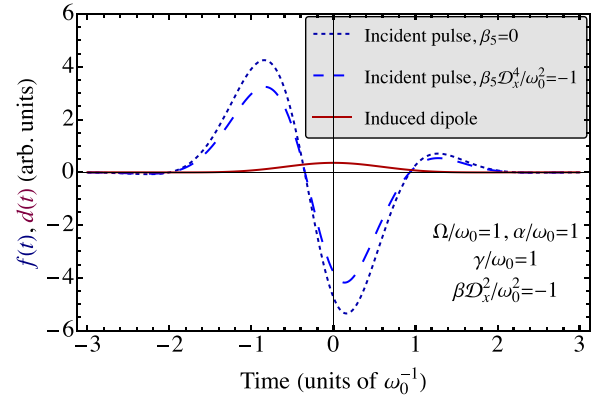

FIG. 2. Dipole $d(t)$ (dark red solid line) taken in the form of Eq. (14) with $\varphi = 0$ and corresponding incident pulse shape $f(t)$ (blue dotted line) and found from Eq. (11) for the parameters where $d_S \neq 0$ and $\int_{-\infty}^{\infty} E_i(t)dt = 0$. The dashed curve is calculated accounting for both third- and fifth-order nonlinearities, $\beta d^3(t) + \beta_5 d^5(t)$, in Eq. (2). Other parameters are indicated in the figure legend.

since for a quantum dot with any damping, $d(t \to \pm\infty) = 0$. Coming back to the case of $\xi = 0$, i.e., neglecting the saturation effects, we obtain from Eqs. (5), (6), and (11)

$$\omega_0^2 d_S + \beta\int_{-\infty}^{\infty} d^3(t)dt = 0. \tag{13}$$

Let us take a time dependence $d(t)$ with $d_S \neq 0$, for example,

$$d(t) = d_0 e^{-\alpha t^2}\cos(\Omega t + \varphi), \tag{14}$$

with the parameters d_0, α, Ω, and $\varphi \neq \pm\pi/2$. Substituting it into Eq. (11), we obtain the field $E_i(t)$ that corresponds to this dipole moment dynamics, as illustrated in Fig. 2; compare the solid curve for $d(t)$ and the dotted curve for $E_i(t)$. The condition (13) of the vanishing zero-frequency component in $E_i(t)$ yields the following relation between the dipole moment and pulse parameters:

$$\frac{\beta}{\omega_0^2}d_0^2 = -\frac{4\sqrt{3}\exp\left(-\frac{\Omega^2}{4\alpha}\right)\cos\varphi}{\exp\left(-\frac{3\Omega^2}{4\alpha}\right)\cos 3\varphi + 3\exp\left(-\frac{\Omega^2}{12\alpha}\right)\cos\varphi}. \tag{15}$$

If Eq. (15) holds (this can be readily done by choosing the amplitude d_0 in Eq. (14) and having other parameters fixed), then there exists such $E_i(t)$ [the explicit expression follows from Eq. (2) and is too cumbersome to be presented here] that Eq. (6) is satisfied while $d_S \neq 0$ in Eq. (5). Then according to Eq. (8), $S_E \neq 0$. Generally, it is possible both for positive and negative coefficients of nonlinearity β. In the particular case in which $\Omega = 0$, $\varphi = 0$, corresponding to a Gaussian shape of the dipole dynamics, Eq. (15) gives $\beta d_0^2 = -\sqrt{3}\omega_0^2$. For a Gaussian profile of the polarization, the nonlinearity coefficient should be negative. The perturbative analysis shows that inclusion of higher order, e.g., $\propto d^5$, in Eq. (2) terms leads only to small quantitative corrections of the results. This is illustrated in Fig. 2 by the dashed curve, which shows $E_i(t)$ producing the same $d(t)$ pulse with $d_S \neq 0$ in the presence of the additional nonlinear term $\beta_5 d^5(t)$ in Eq. (2).
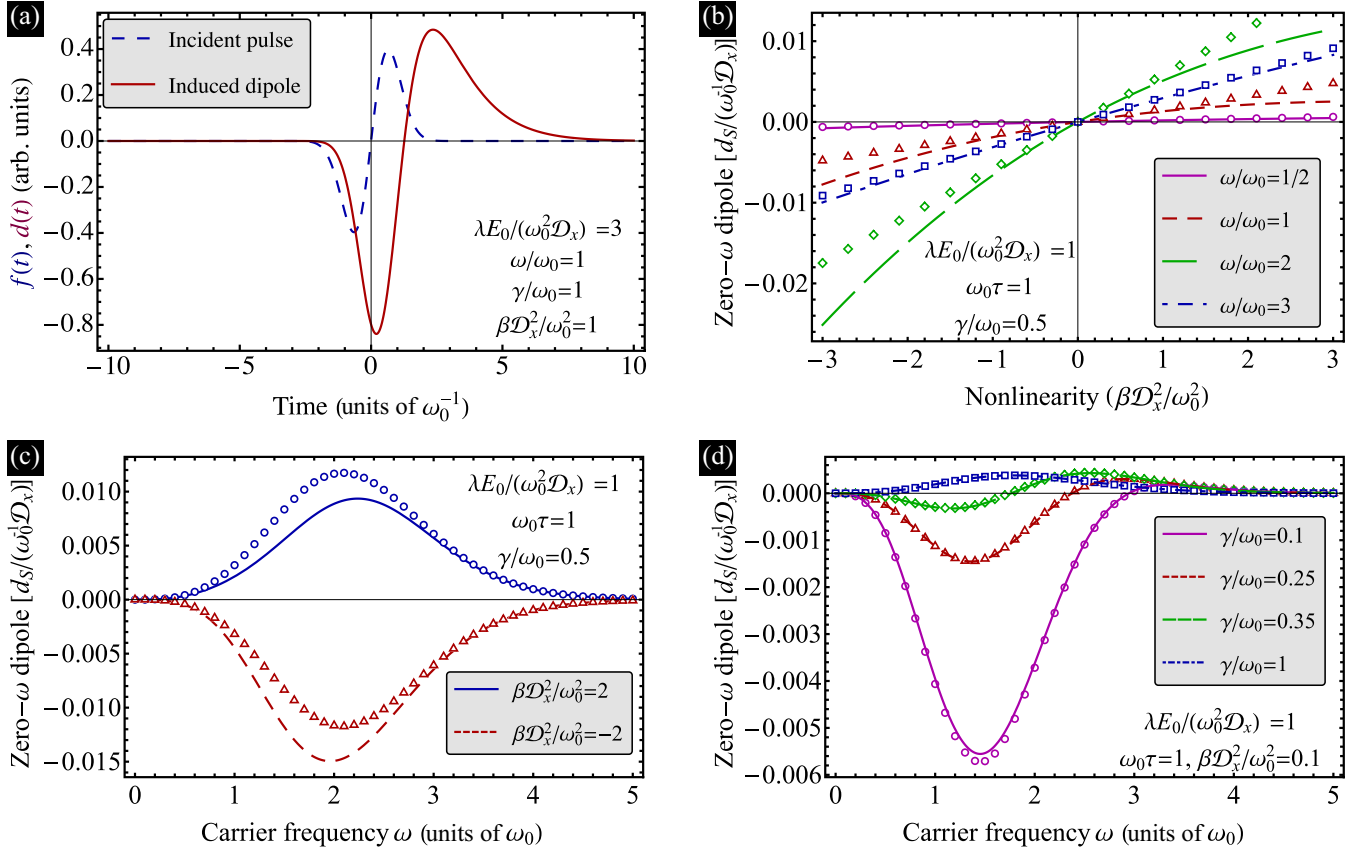
FIG. 3. (a) Incident pulse shape $f(t)$ (blue dashed line) and induced dipole $d(t)$ (dark red solid line) found from numerical solution of Eq. (2). (b)–(d) Zero-frequency component of the dipole moment d_S, Eq. (5), calculated from numerical solution of Eq. (2) (solid lines) and from the third-order perturbation theory, Eq. (20) (dots) as a function of β (b) and ω (c), (d). Other parameters are indicated in the figure legends.

B. Numerical results

The analysis above presents the general proof of the possibility to generate a unipolar pulse (strictly speaking, the pulse with a nonzero area) from the zero-area pulse via a nonlinearity. To demonstrate that a nanocrystal can indeed produce a unipolar field in a more realistic and experimentally relevant case, we consider the incident pulse in the form

$$\boldsymbol{E}_i(t) = \boldsymbol{E}_0 f(t), \qquad (16)$$

where $\boldsymbol{E}_0$ is the amplitude of the incident pulse, and $f(t)$ is the pulse shape function

$$f(t) = \exp\left(-\frac{t^2}{\tau^2}\right) \sin(\omega t). \qquad (17)$$

In the case of multicycle pulses, $\omega\tau \gg 1$, ω is the pulse carrier frequency and τ is the pulse duration. We take the pulse in the form of Eq. (17) to provide the simplest and most straightforward illustration of the effect.

Figure 3 presents the key results of the numerical solution of Eq. (2) with $\xi = 0$. Panel (a) of Fig. 3 shows the incident pulse and the induced dipole moment $d(t)$ of the nanocrystal: The dynamics $d(t)$ is delayed with respect to the pump

pulse, and the response is slightly stretched in time due to the dispersive response of the nanocrystal. The zero-frequency component of the dipole moment d_S, Eq. (5), calculated from the $d(t)$ profile, is shown in Figs. 3(b) and 3(d) by solid lines as a function of the nonlinearity β with the incident field amplitude E_0 being fixed [panel (b) of Fig. 3], and a function of the incident pulse "carrier frequency" ω for different values of the nonlinearity β and damping γ [panels (c) and (d) of Fig. 3, respectively].

Naturally, $d_S \neq 0$ appears only if exciton-exciton interactions are taken into account, $\beta \neq 0$ [Fig. 3(b)]. Indeed, in the linear regime the Fourier components of the incident pulse and dipole are proportional to each other, and the zero-area incident pulse cannot result in the unipolar response. The absolute value $|d_S|$ increases with an increase in $|\beta|$ for other parameters being fixed. The asymmetry in the $d_S(\beta)$ dependence is related to specific asymmetry in the driving force amplitude response of an oscillator with cubic nonlinearity; cf. Ref. [58].

As expected, the zero-frequency dipole component d_S demonstrates resonant behavior as a function of the incident pulse "carrier frequency" [Figs. 3(c) and 3(d)]. The width of resonance is controlled by the inverse pulse duration τ^{-1} and the exciton decay rate γ. Decreasing γ also results in the enhancement of the response as illustrated in Fig. 3(d).

It is instructive to develop a semianalytic approach to describe the formation of d_S based in the perturbation theory.

Introducing the linear polarizability of a nanocrystal in the frequency domain by solving Eq. (2) in the absence of nonlinear terms (cf. Ref. [58]),

$$\chi(\omega) = \frac{\lambda}{\omega_0^2 - 2i\omega\gamma - \omega^2}, \tag{18}$$

we find the induced dipole moment in the form

$$d(t) = \int_{-\infty}^{\infty} \chi(\omega) E_\omega e^{-i\omega t} \frac{d\omega}{2\pi}, \tag{19}$$

where $E_\omega = \int_{-\infty}^{\infty} \exp(i\omega t) E_i(t) dt$ is the Fourier transform of the incident pulse. The cubic nonlinear term $\beta d^3(t)$ in Eq. (2) is then used as a nonlinear driving force. As a result, we obtain in the linear-in-β order

$$d_S = -\frac{\chi(0)\beta}{\lambda} \int_{-\infty}^{\infty} dt \left[\int_{-\infty}^{\infty} \chi(\omega) E_\omega e^{-i\omega t} \frac{d\omega}{2\pi} \right]^3$$
$$= -\frac{\chi(0)\beta}{\lambda} \int_{-\infty}^{\infty} \frac{d\omega_1}{2\pi} \int_{-\infty}^{\infty} \frac{d\omega_2}{2\pi} \chi(\omega_1)\chi(\omega_2)\chi(-\omega_1-\omega_2)$$
$$\times E_{\omega_1} E_{\omega_2} E_{-\omega_1-\omega_2}. \tag{20}$$

The results of d_S calculation by perturbative Eq. (20) are shown in Figs. 3(b)–3(d) by dots. They are in very good agreement with full numerical calculations, particularly if d_S is not too large, $|d_S|/(\omega_0^{-1}\mathcal{D}_x) \lesssim 0.1$, i.e., where the perturbation is indeed small.

Importantly, the perturbative result (20) is not limited to a simple anharmonic oscillator model of the nanocrystal response. It is valid for arbitrary linear susceptibility of a nanocrystal provided that the nonlinearity is βd^3. This expression is particularly useful for determining the generated pulse area in the case in which the incident pulse is strongly off-resonant, $|\omega - \omega_0| \gtrsim \omega_0$, and the single-mode approximation, Eq. (2), becomes insufficient. Particularly, in a quasi-zero-frequency regime where $\omega, \tau^{-1} \ll \omega_0$, the susceptibility $\chi(\omega) \approx \lambda^2/\omega_0^2$, and Eq. (20) is reduced to

$$d_S = -\frac{\beta\lambda^3}{\omega_0^4} \int_{-\infty}^{\infty} E_i^3(t) dt. \tag{21}$$

Interestingly, in this regime d_S vanishes for odd-in-time pulses, $E_i(t) = -E_i(-t)$. [It follows from Eq. (20) that the accounting for $\gamma \neq 0$ is crucial for having $d_S \neq 0$ for odd-in-time pulses where E_ω is imaginary. At zero γ, the susceptibility is real, making the right-hand side of this expression purely imaginary. Since the left-hand side is real, the imaginary part should vanish, resulting in $d_S = 0$ in Eq. (20).] However, $d_S \neq 0$ if the zero-area incident pulse has an asymmetric shape, e.g.,

$$E_i(t) = E_0 \left\{ \exp\left(-\frac{t^2}{\tau^2}\right) \sin\omega_1 t + \exp\left(-\frac{(t-\delta t)^2}{\tau^2}\right) \right.$$
$$\left. \times \sin[\omega_2(t-\delta t)] \right\}. \tag{22}$$

The incident pulse (22) is simply a sum of two zero-area pulses with different "carrier frequencies" $\omega_1 \neq \omega_2$ delayed

by δt. In that case, a zero-frequency component

$$d_S = -\frac{\beta(\lambda E_0)^3}{\omega_0^4} (\omega_2 - \omega_1) \delta t \, \tau \sqrt{\frac{\pi}{3}} \exp\left(-\frac{3}{4}\omega_1^2\tau^2\right)$$
$$\times \left[1 + \exp\left(\frac{2}{3}\omega_1^2\tau^2\right)\left(\frac{2}{3}\omega_1^2\tau - 1\right) \right]. \tag{23}$$

We stress that Eq. (23) is valid at $|\omega_1 - \omega_2| \ll \omega_1, \omega_2, |\delta t| \ll \tau, \omega_{1,2}^{-1}$. The appearance of $d_S \neq 0$ is similar to the ratchet effect in mechanics and in electronic transport where a unidirectional motion appears as a result of asymmetry [59–63]. In the general case, however, as shown in Fig. 3, the unipolar pulse can be produced for odd-in-time incident pulses.

III. DISCUSSION

We have demonstrated that a nonlinear, cubic response of a nanocrystal results in the generation of a unipolar pulse of a dipole moment (5) and, consequently, electric field with a nonzero pulse area, Eq. (8), even if the incident pulse has a zero area. Let us present the estimates of the effect. For large quantum dots, as mentioned in Sec. II A, the nonlinearity coefficient β stems from exciton-exciton interactions. The estimate of the parameter β can be conveniently done based on the exchange interaction model successfully applied to quantum wells, two-dimensional materials, and microcavity structures [64–67]. In this case,

$$\beta \frac{\mathcal{D}_x^2}{2\omega_0} = C \frac{E_B}{\hbar} \left(\frac{a_B}{a}\right)^\delta, \tag{24}$$

where $C \sim 1$ is the numerical constant depending on the geometry of the system, and the exponent δ depends on the geometry of the nanocrystals: $\delta = 2$ for planar dots and $\delta = 3$ for spherical dots. The estimate (24) has a clear physical meaning: if two excitons are within the Bohr radius a_B from each other, than their energy increases by the binding energy E_B. Thus, realistic values of the dimensionless parameter are

$$\beta \frac{\mathcal{D}_x^2}{\omega_0^2} \sim \frac{E_B}{\hbar\omega_0} \left(\frac{a_B}{a}\right)^\delta \sim 10^{-3}, \dots, 10^{-1}. \tag{25}$$

For instance, for planar dots made of transition-metal dichalcogenide monolayers [68] $\delta = 2$, $E_B/\hbar\omega_0 \sim 0.1, \dots, 0.3$, depending on the environment, and the localization radius can be $a \sim 10a_B$. The dimensionless parameter characterizing the field strength can be recast as

$$\frac{\lambda E_0}{\omega_0^2 \mathcal{D}_x} = 2\frac{\mathcal{D}_x E_0}{\hbar\omega_0} = \frac{\mathcal{D}_x}{ea_0} \frac{E_0}{e/a_0}. \tag{26}$$

In the last estimate we introduced a_0, the atomic Bohr radius (of the order of lattice parameter). Thus, the dimensionless field $\lambda E_0/(\omega_0^2 \mathcal{D}_x)$ can be of the order of unity or even larger for the field amplitude E_0 being much smaller than the atomic field e/a_0 due to enhancement of $\mathcal{D}_x$ as compared to the atomic value $\sim ea_0$ discussed in Sec. II A. Thus, values of

$$d_S \sim (10^{-5}, \dots, 10^{-3}) \frac{\mathcal{D}_x}{\omega_0} \tag{27}$$

can be easily attainable; see Fig. 3(d). Combining Eq. (27) with Eq. (8), we obtain the estimate for the generated pulse

area in the form

$$S_E \sim (10^{-5}, \ldots, 10^{-3}) \frac{\mathcal{D}_x}{ea_0} \frac{1\mathrm{Ry}}{\hbar\omega_0} \left(\frac{a_0}{r}\right)^3 \mathcal{S}_{E,0}, \quad (28)$$

where $\mathcal{S}_{E,0} = \hbar/(ea_0)$ is the "atomic" pulse area [13,69], Ry is the Rydberg unit of energy, and we recall that r is the distance from the nanocrystal to the observation point. For $\mathcal{D}_x/(ea_0) \sim (a/a_B)^{3/2} \sim 10$ and $\hbar\omega_0 \sim 1\,\mathrm{eV}$ we have pulses with $S_E/\mathcal{S}_{E,0} \sim (10^{-3}, \ldots, 0.1)(a_0/r)^3$.

Let us now discuss this effect from a more general viewpoint, but remaining in the perturbative regime, introducing the third-order nonlinear susceptibility $\chi^{(3)}(\omega_1, \omega_2, \omega_3)$ in such a way that the induced dipole moment of the nanocrystal $d_\omega = \chi^{(3)}(\omega_1, \omega_2, \omega_3)E_{\omega_1}E_{\omega_2}E_{\omega_3}$ (as before, we omitted Cartesian indices assuming collinear geometry) [70–72]. The zero-frequency component of the polarization can thus be written as [cf. Eq. (20)]

$$d_S = \int_{-\infty}^{\infty} d\omega_1 \int_{-\infty}^{\infty} d\omega_2 \, \chi^{(3)}(\omega_1, \omega_2, -\omega_2 - \omega_3)$$
$$\times E_{\omega_1}E_{\omega_2}E_{-\omega_2-\omega_3}. \quad (29)$$

One can see that for pulses in the form of Eq. (17), the significant d_S can appear only for sufficiently short incident pulses where $\omega\tau$ is not too high. Otherwise, at least one of the Fourier components of the incident field E_{ω_1}, E_{ω_2}, or $E_{-\omega_2-\omega_3}$ in the product (29) is vanishingly small. In this respect, the selection of the incident pulses in the form of a superposition of two pulses, as in Eq. (22) with the frequencies $\omega_2 = 2\omega_1$, is preferable. This $\omega_1 - 2\omega_1$ configuration is also known to be efficient for generation of dc currents in centrosymmetric semiconductors and nanosystems [73–76]. Tailoring the composition of the nanocrystal and its shape, one can achieve a close-to-parabolic confinement potential and equidistant spectrum of size-quantized electronic states that results in a sharp resonance in $\chi^{(3)}(\omega, \omega, -2\omega)$ where $\hbar\omega$ and $2\hbar\omega$ simultaneously coincide with the transition energies $\hbar\omega_0$ and $2\hbar\omega_0$ in the nanocrystal. We stress that allowance for the nanocrystal anisotropy in this mechanism does not bring about novel effects. It can be readily allowed for by including Cartesian subscripts in fields, dipole, and susceptibility. Numerical analysis presented in Appendix B shows that unipolar pulses can be generated also in a framework of a more general two-level model [33,84] which is widely used to describe the optical response of nanocrystals.

Going beyond the third-order nonlinearity, we suggest that efficient generation of unipolar pulses can be achieved in nanocrystals with pronounced quadratic nonlinearity. The latter requires the absence of an inversion center in the point symmetry group of the structure that is usually the case for the conventional III-V or II-VI materials or the interplay of electric and magnetic dipoles or electric quadrupole transitions enabled by the magnetic field of the incident radiation or its wave vector [77,78]. This is an analog of the optical rectification effect [79–82] where the induced dipole $d(t)$ is proportional to $\langle E_i^2(t)\rangle$ with angular brackets denoting the averaging over the fast oscillations at the carrier frequency. While typically in experiments either the radiated electromagnetic field $\propto \dot{d}(t)$ or the transient current $\propto \dot{d}(t)$ is measured, the optical rectification also results in a zero-frequency

component of the polarization,

$$d_S \propto \int_{-\infty}^{\infty} E_i^2(t)dt, \quad (30)$$

and, correspondingly, in the unipolar pulse of electric field, Eq. (8). A significant rectification effect can be achieved for exciton quantum dots for tailored confinement potentials such as semiparabolic ones [83].

Interestingly, in nanocrystals with an asymmetric heteropotential or a built-in electric field, the exciton envelope wave function $\Phi(r_e, r_h)$ introduced in Eqs. (3) and (4) has no definite parity. As a result, the charge distribution in the exciton is asymmetric and the exciton itself possesses a nonzero static dipole moment,

$$\mathcal{D}_0 = e \int (r_e - r_h)|\Phi(r_e, r_h)|^2 dr_h dr_h. \quad (31)$$

If the nanostructure is excited by a short (compared to the exciton lifetime) resonant (with the carrier frequency $\omega = \omega_0$) π-pulse [84–86], then the dipole moment related to the exciton envelope $d(t) = \mathcal{D}_0 \exp(-2\gamma t)$, and a zero-frequency component of the dipole moment takes the form

$$d_S = \frac{\mathcal{D}_0}{2\gamma}. \quad (32)$$

It gives rise, according to Eq. (8), to the unipolar pulse with the electrical pulse area $S_E \sim d_S/r^3$. Taking into account that the electron-hole separation in the exciton can be of the order of the nanocrystal size for asymmetric nanocrystals, the induced pulse area can be estimated as

$$S_E \sim \frac{\mathcal{D}_0}{2\gamma} \frac{1}{r^3} \sim \frac{a}{a_0} \frac{\mathrm{Ry}}{\hbar\gamma} \left(\frac{a_0}{r}\right)^3 \mathcal{S}_{E,0}. \quad (33)$$

Due to a huge factor $\mathrm{Ry}/\hbar\gamma \sim 10^6$ [for typical exciton lifetimes $(2\gamma)^{-1} \sim 100\,\mathrm{ps}$], the pulse area can be comparable to the atomic one, $\mathcal{S}_{E,0}$, near the nanocrystal surface.

In this respect, two related configurations can be preferable from the experimental viewpoint. First, we consider a metallic nanocrystal (plasmonic nanoparticle) that is excited by a short laser pulse, which, due to quadratic nonlinearity, results in opposite velocities of the conduction electrons and lattice ions. It can be achieved, e.g., via the dynamic Hall effect that results in the $\propto [E_i \times B_i]$ current generation [77,87–91]. As a result, after the incident pulse at $t = 0$ the many-body wave function of electrons takes a form [92]

$$\Psi(\{r_i\}, t = 0) = \Psi_0(\{r_i\}) \exp\left(\mathrm{i}\frac{m_0 v_0}{\hbar}\sum_i r_i\right). \quad (34)$$

Here $\{r_i\}$ are the electron coordinates, m_0 is the free-electron mass, $\Psi_0(\{r_i\})$ is the ground-state electronic wave function in the nanocrystal, and v_0 is the velocity of electrons in the reference frame where the nanocrystal lattice is at rest. Assuming that v_0 is small as compared to the atomic velocities $e^2/\hbar$, $|p_{cv}/m_0|$, the exponent in Eq. (34) can be decomposed in the power series. Keeping the linear-in-v_0 contribution, we obtain

$$\Psi(\{r_i\}, t = 0) \approx \Psi_0(\{r_i\})\left(1 + \mathrm{i}\frac{m_0 v_0}{\hbar}\sum_i r_i\right). \quad (35)$$

Note that such a wave function corresponds to a situation in which the nanocrystal had been subjected, at $t = 0$, to an extremely short unipolar electric pulse with the electric area

$$S_{E,0} = \frac{m_0 v_0}{e\hbar}. \tag{36}$$

At the large distance from the nanocrystal, as before, only the dipole component of the fields is important. The zero-frequency component of the induced dipole moment of the nanocrystal reads

$$d_S = \int d(t)dt = \chi(0)S_{E,0}. \tag{37}$$

The area of the generated unipolar pulse is given by Eq. (8). Note that in this model, effectively a conversion of the incident pulse area $S_{E,0}$ to that of the induced one S_E takes place, and the conversion coefficient can be roughly estimated as $\chi(0)/r^3$. Naturally, the effect is largest in metallic particles where $\chi(0) = a^3$, where a is the nanocrystal radius. For dielectric nanoparticles the efficiency is smaller since $\chi(0) = a^3[1 - 3/(2 + \varepsilon)] < a^3$, with ε being the zero-frequency dielectric susceptibility [70].

As a second setting, we consider an interband or impurity-band ionization of a semiconductor nanocrystal where the incident electric field $E_i(t)$ results in conduction- to valence-band transitions [93] (in very strong fields the electrons may leave nanocrystals [38,39], but we do not discuss such a situation here). These photogenerated carriers can be separated by the built-in electric fields or other sources of asymmetry in a nanocrystal yielding $d_S \sim ena^4T$, where n is the density of photogenerated electrons and holes and T is their lifetime.

IV. CONCLUSION

To conclude, we have demonstrated that semiconductor quantum dots can serve as efficient sources of unipolar electromagnetic pulses. The omnipresent third-order nonlinearity related to, e.g., exciton-exciton interaction, converts a zero-area bipolar or multicycle pulse to a unipolar one. The theory of the effect is developed in the framework of the Duffing-like equation describing a nonlinear polarization dynamics in a nanocrystal within a single-mode approximation. Numerical results are well described by a perturbative analytical approach. We have discussed other possible realizations of the unipolar pulse generation related to the second-order non-linearity, the asymmetric shape of the nanocrystal, and the ionization effect. Our estimates show that the effect can be sizable. For instance, for asymmetric nanocrystals the electric area of the generated unipolar pulse can be comparable to the atomic one, $\hbar/(ea_0)$, near the nanocrystal surface. This opens up avenues for experimental observation of the effect and studies of unipolar pulses in a solid-state environment.

APPENDIX A: EFFECT OF A FINITE NANOCRYSTAL SIZE

The model formulated in the main text and, in particular, Eqs. (7) and (8) are derived assuming that the nanocrystal size is negligible and the studied transition corresponds to a point dipole, $d(t)$. Here we demonstrate that accounting for a finite size of a nanocrystal does not change any conclusions of our analysis. We introduce the dipole density $P(r, t)$ (polarization) with $d(t) = \int P(r, t)d^3r$; see Eq. (3). The distribution of $P(r, t)$ in space is described by the envelope function of the electron-hole pair in the nanocrystal [31]. $P(r, t)$ is a smooth function of coordinates that rapidly vanishes at $r > a$, where a is the nanocrystal radius.

Combining Maxwell's equations for the curls of electric and magnetic fields, we obtain [31,41]

$$\Delta E_\omega(r) - \text{grad div}\, E_\omega(r) = -\left(\frac{\omega}{c}\right)^2 [E_\omega(r) + 4\pi P_\omega(r)], \tag{A1}$$

where we introduced the Fourier components of the field $E_\omega(r) = \int E(t)\exp(i\omega t)dt$ and of polarization $P_\omega(r) = \int E(t)\exp(i\omega t)dt$. For simplicity, we neglected the contrast between the background dielectric constant of the nanocrystal and vacuum. It follows from Gauss's law,

$$\text{div}\,[E_\omega(r) + 4\pi P_\omega(r)] = 0, \tag{A2}$$

that grad div $E_\omega(r) = -4\pi$ grad div $P_\omega(r)$. It is instructive to introduce the matrix Green's function of Eq. (A1) in the form [31,94]

$$G_{\alpha\beta}(r) = \left(\delta_{\alpha\beta} + \frac{c^2}{\omega^2}\frac{\partial^2}{\partial r_\alpha \partial r_\beta}\right)\frac{\exp(i\omega r/c)}{4\pi r}, \tag{A3}$$

where $\alpha, \beta = x, y, z$ are the Cartesian components, and we express the field as

$$E_{\omega,\alpha}(r) = \left(\frac{\omega}{c}\right)^2 \int d^3r' G_{\alpha\beta}(r - r')P_{\beta,\omega}(r'). \tag{A4}$$

Equation (A4) can be recast in the form

$$E_\omega(r) = \int d^3r' e^{i\omega R/c}\Bigg[\left(\frac{\omega}{c}\right)^2 \frac{[R \times P_\omega(r')] \times R}{R^3}$$
$$+ \left(\frac{1}{R^3} - \frac{i\omega}{cR^2}\right)\left(\frac{3[R \cdot P_\omega(r')]R}{R^2} - P_\omega(r')\right)\Bigg]$$
$$- \frac{4\pi}{3}P_\omega(r), \tag{A5}$$

where $R = r - r'$.

Note that the last term $\propto P_\omega(r)$ describes the field inside the nanocrystal where $P(r) \neq 0$ (this term describes the field "between" separated charges). By construction, Eq. (A5) satisfies the Maxwell equations and, particularly, Gauss's law, Eq. (A2).

The pulse area is given by the $\omega = 0$ component of Eq. (A5), namely

$$S_E(r) = \int \frac{d^3r'}{R^3}\left(\frac{3[R \cdot P_0(r')]R}{R^2} - P_0(r')\right) - \frac{4\pi}{3}P_0(r). \tag{A6}$$
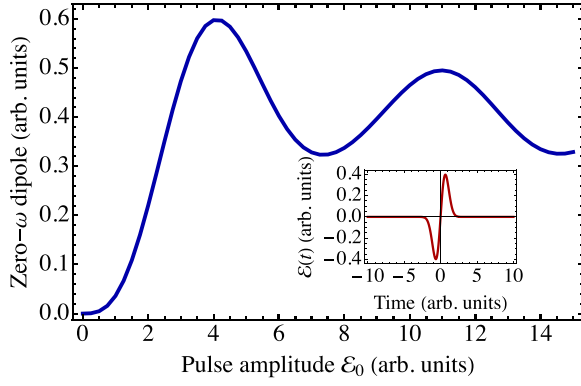
FIG. 4. Zero-frequency component of the dipole moment d_S induced in a "two-level" quantum dot model by a zero-area pulse (shown in the inset) as a function of the incident field amplitude $\mathcal{E}_0$. The incident pulse is taken in the form of Eq. (17) with $\omega = \omega_0$ and $\omega\tau = 1$. In actual numerical calculation, the excited-state damping in the form of $-\gamma\psi_e(t)$ was introduced to the right-hand side of Eq. (B1a) with $\gamma/\omega_0 = 1$.

At large distances from the nanocrystal, $\boldsymbol{P}_\omega(\boldsymbol{r})$ vanishes, $\boldsymbol{R} \approx \boldsymbol{r}$, and integration over $\boldsymbol{r}'$ can be readily performed by virtue of $\boldsymbol{d}_S = \int d^3r' \boldsymbol{P}_0(\boldsymbol{r}')$, resulting in Eq. (7). Naturally, the zero-ω component of $\boldsymbol{E}_\omega$ is given by Eq. (8) of the main text.

In fact, the actual displacements of the charges in the nanocrystal are small and are limited by the nanocrystal size a. Outside the nanocrystal, $\boldsymbol{P}_\omega(\boldsymbol{r})$ decays exponentially in space, because charges are confined by the potential barrier in the nanocrystal: According to Eq. (3), $\boldsymbol{P}_\omega(\boldsymbol{r}) \propto \Phi(\boldsymbol{r}, \boldsymbol{r}) \propto \exp(-\kappa r)$, where κ is related to the barrier height and the carrier's mass, which is typically on the order of Å^{-1} for nanocrystals in free space. At the same time, the electric area

of the induced field $\boldsymbol{E}_S$ decays as $1/r^3$; see Eqs. (A5) and (8). Hence, no macroscopic charge separation and breaking of charge neutrality is needed to generate a field distribution with nonzero $\boldsymbol{S}_E$.

APPENDIX B: TWO-LEVEL MODEL

Here we show that the pulse with nonzero area can be generated by a two-level model which is often used to describe the response of a nanocrystal. In this model, the dynamics is governed by a set of equations

$$i\dot{\psi}_e(t) = \omega_0\psi_e(t) + V(t)\psi_g(t), \tag{B1a}$$

$$i\dot{\psi}_g(t) = V(t)\psi_e(t). \tag{B1b}$$

Here ψ_g and ψ_e are the coefficients of the wave function of the nanocrystal:

$$|\Psi\rangle = \psi_g(t)|0\rangle + \psi_e(t)|\text{exc}\rangle, \tag{B2}$$

where $|0\rangle$ is the ground state of the nanocrystal (no exciton), $|\text{exc}\rangle$ is the excited state of the quantum dot (with exciton), and $V(t) \propto E_i(t)$ is the perturbation induced by the electric field. The dipole moment induced in the quantum dot reads [cf. Eq. (3)]

$$d(t) = -\psi_e(t)\psi_g^*(t)\frac{ie p_{cv}}{\omega_0 m_0}\int \Phi^*(\boldsymbol{r}, \boldsymbol{r})d^3r + \text{c.c.} \tag{B3}$$

Figure 4 shows the dependence of the zero-frequency component of the exciton dipole moment d_S [Eq. (5)] calculated using $d(t)$ in Eq. (B3) found from numerical solution of the system (B1). One can readily see that $d_S \neq 0$ appears in this model as well. The oscillations of d_S as a function of E_0 result from the Rabi effect inherent to two-level systems. Naturally, in agreement with general analysis in the main text, $d_S \propto E_0^3$ for weak incident pulses.

[1] https://www.nobelprize.org/prizes/chemistry/1999/summary/.

[2] https://www.nobelprize.org/prizes/physics/2023/summary/.

[3] T. Gaumnitz, A. Jain, Y. Pertot, M. Huppert, I. Jordan, F. Ardana-Lamas, and H. J. Wörner, Streaking of 43-attosecond soft-X-ray pulses generated by a passively CEP-stable mid-infrared driver, Opt. Express **25**, 27506 (2017).

[4] R. R. Jones, D. You, and P. H. Bucksbaum, Ionization of Rydberg atoms by subpicosecond half-cycle electromagnetic pulses, Phys. Rev. Lett. **70**, 1236 (1993).

[5] D. Dimitrovski, E. A. Solov'ev, and J. S. Briggs, Ionization and recombination in attosecond electric field pulses, Phys. Rev. A **72**, 043411 (2005).

[6] A. Lugovskoy and I. Bray, Almost sudden perturbation of a quantum system with ultrashort electric pulses, Phys. Rev. A **77**, 023420 (2008).

[7] A. Emmanouilidou and T. Uzer, Electron stripping and reattachment at atomic centers using attosecond half-cycle pulses, Phys. Rev. A **77**, 063416 (2008).

[8] M. Klaiber, D. Dimitrovski, and J. S. Briggs, Magnus expansion for laser-matter interaction: Application to generic few-cycle laser pulses, Phys. Rev. A **79**, 043402 (2009).

[9] D. Dimitrovski, M. Førre, and L. B. Madsen, Strong-field short-pulse nondipole dynamics, Phys. Rev. A **80**, 053412 (2009).

[10] N. N. Rosanov, Interactions of intense extremely short pulses with quantum objects, Opt. Spectrosc. **124**, 72 (2018).

[11] R. M. Arkhipov, A. V. Pakhomov, M. V. Arkhipov, I. Babushkin, A. Demircan, U. Morgner, and N. N. Rosanov, Unipolar subcycle pulse-driven nonresonant excitation of quantum systems, Opt. Lett. **44**, 1202 (2019).

[12] R. Arkhipov, A. Pakhomov, M. Arkhipov, A. Demircan, U. Morgner, N. Rosanov, and I. Babushkin, Selective ultrafast control of multi-level quantum systems by subcycle and unipolar pulses, Opt. Express **28**, 17020 (2020).

[13] N. Rosanov, D. Tumakov, M. Arkhipov, and R. Arkhipov, Criterion for the yield of micro-object ionization driven by few- and subcycle radiation pulses with nonzero electric area, Phys. Rev. A **104**, 063101 (2021).

[14] A. Pakhomov, M. Arkhipov, N. Rosanov, and R. Arkhipov, Ultrafast control of vibrational states of polar molecules with subcycle unipolar pulses, Phys. Rev. A **105**, 043103 (2022).

[15] Y. Gao, T. Drake, Z. Chen, and M. F. DeCamp, Half-cycle-pulse terahertz emission from an ultrafast laser plasma in a solid target, Opt. Lett. **33**, 2776 (2008).

[16] H. C. Wu and J. Meyer-ter Vehn, Giant half-cycle attosecond pulses, Nat. Photon. **6**, 304 (2012).

[17] M. T. Hassan, T. T. Luu, A. Moulet, O. Raskazovskaya, P. Zhokhov, M. Garg, N. Karpowicz, A. M. Zheltikov, V. Pervak,

F. Krausz, and E. Goulielmakis, Optical attosecond pulses and tracking the nonlinear response of bound electrons, Nature (London) **530**, 66 (2016).

[18] G. Naumenko and M. Shevelev, First indication of the coherent unipolar diffraction radiation generated by relativistic electrons, J. Instrum. **13**, C05001 (2018).

[19] J. Xu, B. Shen, X. Zhang, Y. Shi, L. Ji, L. Zhang, T. Xu, W. Wang, X. Zhao, and Z. Xu, Terawatt-scale optical half-cycle attosecond pulses, Sci. Rep. **8**, 2669 (2018).

[20] I. E. Ilyakov, B. V. Shishkin, E. S. Efimenko, S. B. Bodrov, and M. I. Bakunov, Experimental observation of optically generated unipolar electromagnetic precursors, Opt. Express **30**, 14978 (2022).

[21] M. V. Arkhipov, A. N. Tsypkin, M. O. Zhukova, A. O. Ismagilov, A. V. Pakhomov, N. N. Rosanov, and R. M. Arkhipov, Experimental determination of the unipolarity of pulsed terahertz radiation, JETP Lett. **115**, 1 (2022).

[22] R. Arkhipov, M. Arkhipov, and N. Rosanov, Unipolar light: existence, generation, propagation, and impact on microobjects, Quantum Electron. **50**, 801 (2020).

[23] N. N. Rosanov, Unipolar pulse of an electromagnetic field with uniform motion of a charge in a vacuum, Phys. Usp. **66**, 1059 (2023).

[24] A. I. Ekimov and A. A. Onushchenko, Quantum size effect in three-dimensional microscopic semiconductor crystals, JETP Lett. **34**, 343 (1981).

[25] R. Rossetti, S. Nakahara, and L. E. Brus, Quantum size effects in the redox potentials, resonance Raman spectra, and electronic spectra of CdS crystallites in aqueous solution, J. Chem. Phys. **79**, 1086 (1983).

[26] L. Goldstein, F. Glas, J. Y. Marzin, M. N. Charasse, and G. Le Roux, Growth by molecular beam epitaxy and characterization of InAs/GaAs strained-layer superlattices, Appl. Phys. Lett. **47**, 1099 (1985).

[27] C. B. Murray, C. R. Kagan, and M. G. Bawendi, Synthesis and characterization of monodisperse nanocrystals and close-packed nanocrystal assemblies, Annu. Rev. Mater. Sci. **30**, 545 (2000).

[28] A. L. Efros and M. Rosen, The electronic structure of semiconductor nanocrystals, Annu. Rev. Mater. Sci. **30**, 475 (2000).

[29] D. Bimberg, M. Grundmann, and N. N. Ledenstov, *Quantum Dot Heterostructures* (Wiley-VCH Verlag, Chichester, UK, 1999).

[30] *Semiconductor Quantum Dots: Physics, Spectroscopy and Applications*, edited by Y. Masumoto and T. Takagahara (Springer, Berlin, 2002).

[31] E. L. Ivchenko, *Optical Spectroscopy of Semiconductor Nanostructures* (Alpha Science, Harrow, UK, 2005).

[32] O. Gywat, H. Krenner, and J. Berezovsky, *Spins in Optically Active Quantum Dots: Concepts and Methods* (Wiley, Chichester, UK, 2010).

[33] M. Glazov, *Electron & Nuclear Spin Dynamics in Semiconductor Nanostructures*, Series on Semiconductor Science and Technology (Oxford University Press, Oxford, 2018).

[34] A. L. Efros and L. E. Brus, Nanocrystal quantum dots: From discovery to modern development, ACS Nano **15**, 6192 (2021).

[35] F. Montanarella and M. V. Kovalenko, Three millennia of nanocrystals, ACS Nano **16**, 5085 (2022).

[36] L. Brus, Quantum crystallites and nonlinear optics, Appl. Phys. A **53**, 465 (1991).

[37] D. Englund, I. Fushman, A. Faraon, and J. Vučković, Quantum dots in photonic crystals: From quantum information processing to single photon nonlinear optics, Photon. Nanostruct.—Fundament. Appl. **7**, 56 (2009).

[38] M. F. Ciappina, J. A. Pérez-Hernández, A. S. Landsman, W. A. Okell, S. Zherebtsov, B. Förg, J. Schötz, L. Seiffert, T. Fennel, T. Shaaran, T. Zimmermann, A. Chacón, R. Guichard, A. Zaïr, J. W. G. Tisch, J. P. Marangos, T. Witting, A. Braun, S. A. Maier, L. Roso *et al.*, Attosecond physics at the nanoscale, Rep. Prog. Phys. **80**, 054401 (2017).

[39] L. Seiffert, S. Zherebtsov, M. F. Kling, and T. Fennel, Strong-field physics with nanospheres, Adv. Phys.: X **7**, 2010595 (2022).

[40] A. N. Poddubny, M. M. Glazov, and N. S. Averkiev, Collective effects in emission of localized excitons strongly coupled to a microcavity photon, New J. Phys. **15**, 025016 (2013).

[41] M. M. Glazov, E. L. Ivchenko, A. N. Poddubny, and G. Khitrova, Purcell factor in small metallic cavities, Phys. Solid. State **53**, 1753 (2011).

[42] K. Leo, M. Wegener, J. Shah, D. S. Chemla, E. O. Göbel, T. C. Damen, S. Schmitt-Rink, and W. Schäfer, Effects of coherent polarization interactions on time-resolved degenerate four-wave mixing, Phys. Rev. Lett. **65**, 1340 (1990).

[43] F. P. Laussy, M. M. Glazov, A. Kavokin, D. M. Whittaker, and G. Malpuech, Statistics of excitons in quantum dots and their effect on the optical emission spectra of microcavities, Phys. Rev. B **73**, 115343 (2006).

[44] A. L. Efros and A. L. Efros, Interband light absorption in semiconductor spheres, Sov. Phys. Semicond. **16**, 772 (1982).

[45] M. A. Semina, R. A. Sergeev, and R. A. Suris, Localization of electron-hole complexes at fluctuations of interfaces of quantum dots, Semiconductors **40**, 1338 (2006).

[46] E. I. Rashba and G. E. Gurgenishvili, Edge absorption theory in semiconductors, Sov. Phys. Solid State **4**, 759 (1962).

[47] Y. Fu, S. Hellström, and H. Ågren, Nonlinear optical properties of quantum dots: excitons in nanostructures, J. Nonlin. Opt. Phys. Mater. **18**, 195 (2009).

[48] E. V. Melik-Gaykazyan, M. R. Shcherbakov, A. S. Shorokhov, I. Staude, I. Brener, D. N. Neshev, Y. S. Kivshar, and A. A. Fedyanin, Third-harmonic generation from mie-type resonances of isolated all-dielectric nanoparticles, Philos. Trans. R. Soc. A **375**, 20160281 (2017).

[49] Y. Kivshar, Nonlinear Mie-resonant meta-optics and nanophotonics, in *Nonlinear Optics (NLO), OSA Technical Digest* (Optica Publishing Group, 2019), paper NW2A.7.

[50] M. Kauranen and A. V. Zayats, Nonlinear plasmonics, Nat. Photon. **6**, 737 (2012).

[51] J. Obermeier, T. Schumacher, and M. Lippitz, Nonlinear spectroscopy of plasmonic nanoparticles, Adv. Phys.: X **3**, 1454341 (2018).

[52] N. C. Panoiu, W. E. I. Sha, D. Y. Lei, and G.-C. Li, Nonlinear optics in plasmonic nanostructures, J. Opt. **20**, 083001 (2018).

[53] P. Kaw, G. Schmidt, and T. Wilcox, Filamentation and trapping of electromagnetic radiation in plasmas, Phys. Fluids **16**, 1522 (1973).

[54] P. Ginzburg, A. Hayat, E. Feigenbaum, N. Berkovitch, and M. Orenstein, Nonlinear surface plasmon polaritons and the ponderomotive force, in *LEOS 2007—IEEE Lasers and Electro-Optics Society Annual Meeting Conference Proceedings* (IEEE, Piscataway, NJ, 2007), pp. 624–625.

[55] M. Born and E. Wolf, *Principles of Optics: Electromagnetic Theory of Propagation, Interference and Diffraction of Light* (Cambridge University Press, Cambridge, UK, 1999).

[56] L. Landau and E. Lifshitz, *The Classical Theory of Fields* (Butterworth-Heinemann, Oxford, 1975).

[57] N. N. Rosanov, Transportation of extremely short radiation pulses in a waveguide with a nonsimply connected cross section, Opt. Spectrosc. **127**, 1050 (2019).

[58] L. Landau and E. Lifshitz, *Mechanics* (Butterworth-Heinemann, Oxford, 1976).

[59] H. Linke, T. E. Humphrey, A. Löfgren, A. O. Sushkov, R. Newbury, R. P. Taylor, and P. Omling, Experimental tunneling ratchets, Science **286**, 2314 (1999).

[60] P. Reimann, Brownian motors: noisy transport far from equilibrium, Phys. Rep. **361**, 57 (2002).

[61] P. Hänggi, F. Marchesoni, and F. Nori, Brownian motors, Ann. Phys. (Leipzig) **517**, 7 (2005).

[62] A. V. Nalitov, L. E. Golub, and E. L. Ivchenko, Ratchet effects in two-dimensional systems with a lateral periodic potential, Phys. Rev. B **86**, 115301 (2012).

[63] C. Drexler, S. A. Tarasenko, P. Olbrich, J. Karch, M. Hirmer, F. Muller, M. Gmitra, J. Fabian, R. Yakimova, S. Lara-Avila, S. Kubatkin, M. Wang, R. Vajtai, P. Ajayan, J. Kono, and S. D. Ganichev, Magnetic quantum ratchet effect in graphene, Nat. Nano. **8**, 104 (2013).

[64] C. Ciuti, V. Savona, C. Piermarocchi, A. Quattropani, and P. Schwendimann, Role of the exchange of carriers in elastic exciton-exciton scattering in quantum wells, Phys. Rev. B **58**, 7926 (1998).

[65] F. Tassone and Y. Yamamoto, Exciton-exciton scattering dynamics in a semiconductor microcavity and stimulated scattering into polaritons, Phys. Rev. B **59**, 10830 (1999).

[66] M. M. Glazov, H. Ouerdane, L. Pilozzi, G. Malpuech, A. V. Kavokin, and A. D'Andrea, Polariton-polariton scattering in microcavities: A microscopic theory, Phys. Rev. B **80**, 155306 (2009).

[67] V. Shahnazaryan, I. Iorsh, I. A. Shelykh, and O. Kyriienko, Exciton-exciton interaction in transition-metal dichalcogenide monolayers, Phys. Rev. B **96**, 115409 (2017).

[68] G. Wang, A. Chernikov, M. M. Glazov, T. F. Heinz, X. Marie, T. Amand, and B. Urbaszek, *Colloquium:* Excitons in atomically thin transition metal dichalcogenides, Rev. Mod. Phys. **90**, 021001 (2018).

[69] R. M. Arkhipov, M. V. Arkhipov, A. V. Pakhomov, and N. N. Rosanov, Atomic scale of an electrical area for unipolar light pulses, JETP Lett. **114**, 129 (2021).

[70] L. Landau and E. Lifshitz, *Electrodynamics of Continuous Media* (Butterworth-Heinemann, Oxford, 2004), Vol. 8.

[71] Y.-R. Shen, *The Principles of Nonlinear Optics* (Wiley-Interscience, New York, 1984).

[72] R. W. Boyd, *Nonlinear Optics* (Academic, Amsterdam, 2003).

[73] G. M. Shmelev, N. H. Shon, and G. I. Tsurkan, Photostimulated even acousto-electric effect, Izv. Vyssh. Uchebn. Zaved. Fiz. **28**, 84 (1985).

[74] M. V. Entin, Theory of coherent photogalvanic effect, Sov. Phys. Semicond. **23**, 664 (1989).

[75] D. Sun, C. Divin, J. Rioux, J. E. Sipe, C. Berger, W. A. de Heer, P. N. First, and T. B. Norris, Coherent control of ballistic photocurrents in multilayer epitaxial graphene using quantum interference, Nano Lett. **10**, 1293 (2010).

[76] D. Sun, J. Rioux, J. E. Sipe, Y. Zou, M. T. Mihnev, C. Berger, W. A. de Heer, P. N. First, and T. B. Norris, Evidence for interlayer electronic coupling in multilayer epitaxial graphene from polarization-dependent coherently controlled photocurrent generation, Phys. Rev. B **85**, 165427 (2012).

[77] S. Ganichev and W. Prettl, *Intense Terahertz Excitation of Semiconductors* (Oxford Science, Oxford, UK, 2006).

[78] M. M. Glazov and S. D. Ganichev, High frequency electric field induced nonlinear effects in graphene, Phys. Rep. **535**, 101 (2014).

[79] M. Bass, P. A. Franken, and J. F. Ward, Optical rectification, Phys. Rev. **138**, A534 (1965).

[80] V. I. Belinicher, E. L. Ivchenko, and G. E. Pikus, Transient photocurrent in gyrotropic crystals, Sov. Phys. - Semicond. **20**, 558 (1986).

[81] P. Smith, D. Auston, and M. Nuss, Subpicosecond photoconducting dipole antennas, IEEE J. Quantum Electron. **24**, 255 (1988).

[82] X.-C. Zhang, B. B. Hu, J. T. Darrow, and D. H. Auston, Generation of femtosecond electromagnetic pulses from semiconductor surfaces, Appl. Phys. Lett. **56**, 1011 (1990).

[83] S. Baskoutas, E. Paspalakis, and A. F. Terzis, Effects of excitons in nonlinear optical rectification in semiparabolic quantum dots, Phys. Rev. B **74**, 153306 (2006).

[84] A. Greilich, R. Oulton, E. A. Zhukov, I. A. Yugova, D. R. Yakovlev, M. Bayer, A. Shabaev, A. L. Efros, I. A. Merkulov, V. Stavarache, D. Reuter, and A. Wieck, Optical control of spin coherence in singly charged (In,Ga)As/GaAs quantum dots, Phys. Rev. Lett. **96**, 227401 (2006).

[85] Y. Benny, S. Khatsevich, Y. Kodriano, E. Poem, R. Presman, D. Galushko, P. M. Petroff, and D. Gershoni, Coherent optical writing and reading of the exciton spin state in single quantum dots, Phys. Rev. Lett. **106**, 040504 (2011).

[86] D. Cogan, Z.-E. Su, O. Kenneth, and D. Gershoni, Deterministic generation of indistinguishable photons in a cluster state, Nat. Photon. **17**, 324 (2023).

[87] H. M. Barlow, Application of the Hall effect in a semiconductor to the measurement of power in an electromagnetic field, Nature (London) **173**, 41 (1954).

[88] B. I. Sturman and V. M. Fridkin, *The Photovoltaic and Photorefractive Effects in Non-centrosymmetric Materials* (Gordon and Breach, New York, 1992).

[89] V. L. Gurevich, R. Laiho, and A. V. Lashkul, Photomagnetism of metals, Phys. Rev. Lett. **69**, 180 (1992).

[90] R. Hertel, Theory of the inverse Faraday effect in metals, J. Magn. Magn. Mater. **303**, L1 (2006).

[91] J. Karch, P. Olbrich, M. Schmalzbauer, C. Zoth, C. Brinsteiner, M. Fehrenbacher, U. Wurstbauer, M. M. Glazov, S. A. Tarasenko, E. L. Ivchenko, D. Weiss, J. Eroms, R. Yakimova, S. Lara-Avila, S. Kubatkin, and S. D. Ganichev, Dynamic Hall effect driven by circularly polarized light in a graphene layer, Phys. Rev. Lett. **105**, 227402 (2010).

[92] L. D. Landau and E. M. Lifshitz, *Quantum Mechanics: Non-Relativistic Theory* (Butterworth-Heinemann, Oxford, 1977).

[93] L. V. Keldysh, Ionization in the field of a strong electromagnetic wave, JETP **20**, 1307 (1965).

[94] F. Thiele, Ch. Fuchs, and R. v. Baltz, Optical absorption in semiconductor quantum dots: Nonlocal effects, Phys. Rev. B **64**, 205309 (2001).